

## New functional assay of P-glycoprotein activity using Hoechst 33342

Henrik Müller,<sup>a</sup> Werner Klinkhammer,<sup>a</sup> Christoph Globisch,<sup>a</sup> Matthias U. Kassack,<sup>a</sup> Ilza K. Pajeva<sup>a,b</sup> and Michael Wiese<sup>a,\*</sup>

<sup>a</sup>*Institute of Pharmacy, University of Bonn, An der Immenburg 4, 53121 Bonn, Germany*

<sup>b</sup>*Center of Biomedical Engineering, Bulgarian Academy of Sciences, Acad. G. Bonchev Str. Bl. 105, 1113 Sofia, Bulgaria*

Received 11 January 2007; revised 11 June 2007; accepted 6 July 2007

Available online 21 August 2007

**Abstract**—In this study we describe a simplified, HTS-capable functional assay for the multidrug resistance (MDR) transporter P-glycoprotein (P-gp) based on its substrate Hoechst 33342. The physicochemical properties of Hoechst 33342 and the enormous milieu dependency of its fluorescence intensity allowed performing the assay in a homogeneous manner. This new assay served as an effective tool to estimate the potency of 10 well recognized P-gp substrates and modulators. Further, the potency of these compounds was also estimated in the calcein AM assay. The Hoechst 33342 and calcein AM assays yielded significantly comparable results for all compounds tested. Principal component analysis (PCA) applied to literature data on inhibition of P-gp activity and our results obtained in the Hoechst 33342 and calcein AM assay indicated similarity of compared functional transport assays. However, no correlation could be detected between these functional assays and the ATPase activity assay.  
© 2007 Elsevier Ltd. All rights reserved.

### 1. Introduction

Multidrug resistance (MDR) is a major obstacle for successful and effective chemotherapeutic treatment of cancer diseases. MDR involves multiple mechanisms and the most important ones are associated with the overexpression of various members of the ATP-binding cassette (ABC)-family of transport proteins. Among them, P-glycoprotein (P-gp) is the most extensively studied. It belongs to the ABC subfamily B and is encoded by the ABCB1 gene. P-gp is naturally expressed in excreting organs, epithelial membranes and seems to play a key role in the xenobiotic protection of the cells.<sup>1</sup> In tumor cells the protein recognizes a large variety of different antineoplastic agents (e.g., anthracyclines, vinca alkaloids, taxanes) as substrates for an ATP-dependent efflux, consequently minimizing their intracellular concentrations.<sup>2</sup> Many compounds have been investigated for their ability to inhibit the P-gp function, thus leading to development of several generations of MDR modulators.<sup>3</sup>

Still a matter of debate is the number and location of the binding site(s) of P-gp. According to the model of Shapiro and Ling,<sup>4</sup> P-gp has at least two different transport binding sites. One binds the dye Hoechst 33342 and is called the H-site. It interacts with the other site that binds rhodamine 123 (R-site) in a cooperative manner. This cooperativity is supported by the results of Kondratov et al.<sup>5</sup> They found a dramatic stimulation of P-gp activity against doxorubicin, daunorubicin, and rhodamine 123 by small molecules (QB-compounds) that presumably bind to the H-site. Based on radioligand-binding studies, Martin et al. investigated the type of interaction between different P-gp substrates and modulators.<sup>6</sup> They reported a competitive interaction of the 3rd generation MDR modulator XR9576 and Hoechst 33342, thus presuming a common binding site of these compounds, but could not assign a particular binding site for rhodamine 123. Roe et al. investigated a series of analogues of XR9576 (XR-type MDR modulators) and observed a strong inhibitory effect for a number of them in a [<sup>3</sup>H]daunorubicin accumulation assay.<sup>7</sup> Their results imply that the XR-compounds may influence the binding of daunorubicin that has been suggested to interact with the R-site of P-gp.<sup>4</sup> Thus the so far published data about the binding properties of the XR-type modulators raise the question if these com-

**Keywords:** P-Glycoprotein; Multidrug Resistance; Hoechst 33342; 3rd generation modulators.

\* Corresponding author. Tel.: +49 228 735213; fax: +49 228 737929; e-mail: [mwiese@uni-bonn.de](mailto:mwiese@uni-bonn.de)

pounds interact with the R- or the H-site or affect both binding sites of P-gp. This question addresses also the possibility suggested by some authors for existence of a large drug binding pocket that can accommodate more than one drug molecule.<sup>8–10</sup>

Obviously it is of interest to estimate the activity of new generation P-gp modulators in relation to substrates that possibly interact with either of the binding sites of P-gp. Therefore we developed a Hoechst 33342-based functional assay that could allow the determination of P-gp activity relating to the H-site. Besides cyclosporine A, verapamil, vinblastine and five other P-gp substrates and inhibitors, three 3rd generation MDR modulators, XR9577, XR9456, and WK-X-34 were examined in the new Hoechst assay. The data obtained were compared to activity data generated in the well-known calcein AM assay. Further the results of these assays were compared to several other functional assays, using different substrates to determine P-gp function, and to the ATPase activity assay, collected from the literature.

Our results suggest that the transport functional assays based on different P-gp substrates may produce similar results thus hampering the correct identification of the substrate binding sites. In contrast to these functional assays the ATPase activity measurements may provide different information for the characterization of P-gp.

## 2. Results

### 2.1. Resistance factors and P-gp expression

The adriamycin-resistant cell line A2780adr is reported to highly overexpress the ABCB1 gene product P-gp.<sup>11–15</sup> In the cell line used P-gp expression was demonstrated by RT-PCR analysis and by protein surface analysis with the 17F9 monoclonal P-gp antibody and flow cytometry.<sup>16–18</sup> The absence of the ABCG2 gene product BCRP was proven by the specific antibody BXP-21.<sup>16,19</sup> Additionally drug-resistance factors against a series of cytotoxic drugs were determined. Table 1 shows pIC<sub>50</sub>-values and resistance factors of the tested compounds in A2780adr and parental A2780 cells. Our data are comparable with resistance factors for the P-gp substrate doxorubicin reported in the literature.<sup>11,15</sup> As seen from the table the overexpression of

the ABCB1 gene causes also cross-resistance to other P-gp substrates, for example, colchicin, docetaxel, vinblastine reported in the literature.<sup>20</sup> In accordance with literature data cisplatin was characterized as a non-P-gp substrate.<sup>13</sup> Not surprisingly, oxaliplatin could also be classified as a non-P-gp substrate. IC<sub>50</sub>-values of cisplatin and oxaliplatin were not significantly different in A2780 and A2780adr cells.

The overexpression of P-gp in A2780adr cells was further proven by surface protein expression analysis using a selective FITC-labeled P-gp antibody and flow cytometry.<sup>17,18</sup> A big difference between the fluorescence intensities of the bound FITC antibody in A2780adr and A2780 cells was detected: A2780 ( $5.77 \pm 1.33$ ) and A2780adr ( $48.79 \pm 2.65$ ). The fluorescence intensity of A2780 cells was comparable to the background fluorescence intensity, thus the level of P-gp expression was negligible.

### 2.2. Hoechst 33342 assay

The newly proposed assay is based on two main aspects: the dependency of the fluorescence intensity of Hoechst 33342 on the environment and the high distribution coefficient of the substrate into the cell membrane.

In the standard assay, Hoechst 33342 (final concentration 5  $\mu$ M) is added to the cells after preincubation with modulators or substrates. After a 20 min incubation period, the cells are washed three times with KHP, thereafter the fluorescence is measured immediately.

However, it is well known that the fluorescence intensity increases enormously if Hoechst 33342 is bound to the DNA or is localized in a lipophilic environment like the plasma membrane.<sup>21–24</sup> This milieu dependency of the fluorescence intensity of Hoechst 33342 prompted us to investigate the possibility to perform the assay in a different way.

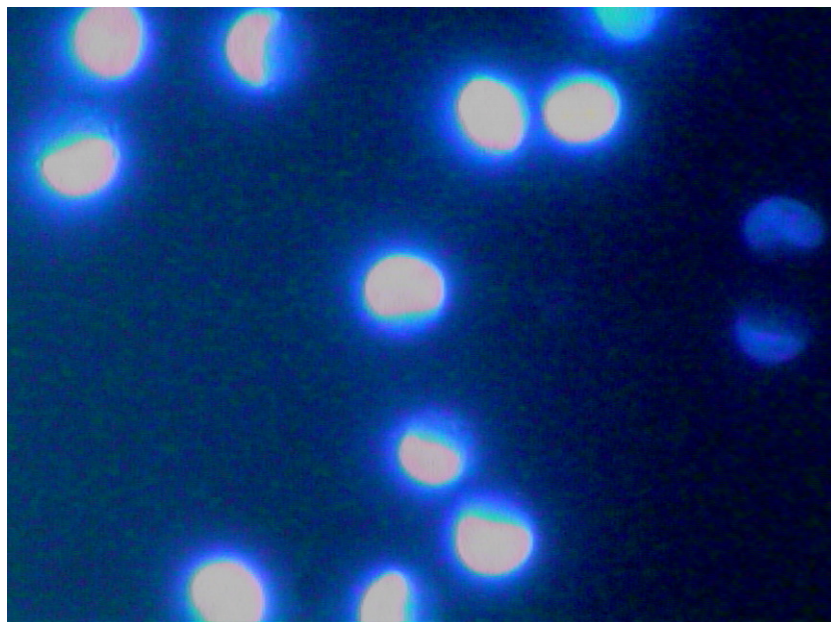
Applying fluorescence microscopy the milieu dependency of the fluorescence intensity of Hoechst 33342 becomes obvious. Figure 1 shows A2780adr cells in the presence of 5  $\mu$ M Hoechst 33342. Even without inhibition of P-gp, the cellular fluorescence is far brighter than the extracellular one. The strong increase in fluorescence intensity in a lipophilic environment combined with the high distribution coefficient of Hoechst 33342 into the plasma membrane explains the observed increase in fluorescence in presence of cells although their volume is very small compared to the total volume. These observations provide the possibility to exclude time-consuming washing steps.

Figure 2 depicts two concentration–response curves for the modulator XR9577: open circle symbols refer to the standard Hoechst assay, and closed circle symbols to the new Hoechst assay. Comparing pIC<sub>50</sub>-values and Hill-coefficients ( $n_H$ ) of both concentration–response curves with an *F*-test, no significant difference was detected: in the standard assay pIC<sub>50</sub> =  $6.36 \pm 0.07$  and  $n_H$  =  $2.27 \pm 0.26$ ; in the new assay pIC<sub>50</sub> =

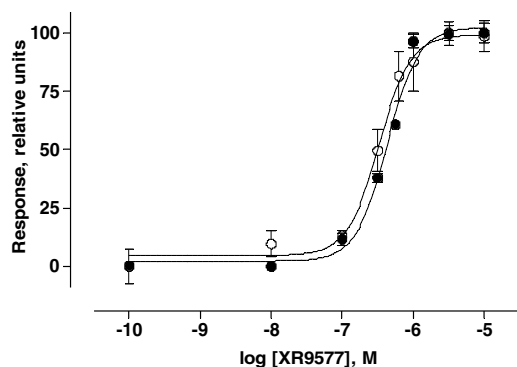
**Table 1.** MTT assay based pIC<sub>50</sub>-values and resistance factors for different cytostatics in the cell lines A2780adr and A2780

Compound	A2780adr pIC <sub>50</sub> $\pm$ SD	A2780 pIC <sub>50</sub> $\pm$ SD	Resistance factor $\pm$ SD
Cisplatin	4.90 $\pm$ 0.12	5.29 $\pm$ 0.07	2.47 $\pm$ 1.34
Colchicin	6.43 $\pm$ 0.20	7.64 $\pm$ 0.04	16.28 $\pm$ 1.61
Daunorubicin	4.73 $\pm$ 0.14	6.93 $\pm$ 0.09	158.70 $\pm$ 1.47
Docetaxel	7.06 $\pm$ 0.04	8.31 $\pm$ 0.11	17.80 $\pm$ 1.33
Doxorubicin	4.87 $\pm$ 0.26	7.03 $\pm$ 0.23	145.55 $\pm$ 2.25
Hoechst 33342	4.42 $\pm$ 0.10	5.72 $\pm$ 0.05	20.14 $\pm$ 1.29
Oxaliplatin	5.71 $\pm$ 0.18	5.60 $\pm$ 0.09	0.76 $\pm$ 1.59
Rhodamine 123	3.91 $\pm$ 0.14	5.72 $\pm$ 0.03	63.68 $\pm$ 1.39
Vinblastine	5.55 $\pm$ 0.06	7.21 $\pm$ 0.13	45.96 $\pm$ 1.39

Presented are means  $\pm$  SD.



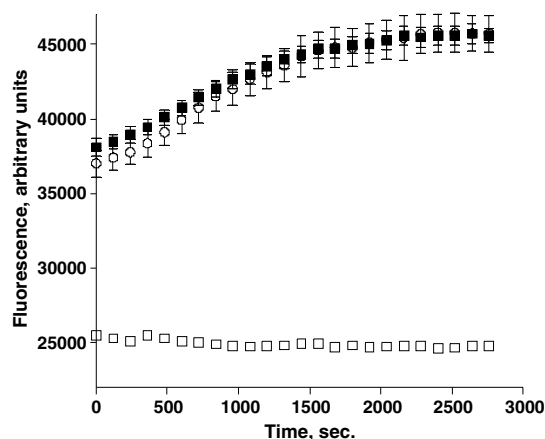
**Figure 1.** A2780adr cells stained with Hoechst 33342 (5  $\mu$ M) and viewed under the fluorescence microscope. The remarkable, significant difference between the intracellular and extracellular fluorescence intensity becomes obvious.



**Figure 2.** Concentration–response curves for XR9577 in A2780adr cells obtained with the standard Hoechst assay (open circles) and the new Hoechst assay (closed circles). In comparison to the standard Hoechst assay, the new Hoechst assay avoids three additional washing steps to remove extracellular Hoechst 33342. Data presented are average  $\pm$  SE from one typical experiment with three replicates belonging to a series of three independent experiments: standard assay:  $\text{pIC}_{50} = 6.36 \pm 0.07$ ,  $n_H = 2.27 \pm 0.26$ , new assay:  $\text{pIC}_{50} = 6.49 \pm 0.08$ ,  $n_H = 1.96 \pm 0.53$ .

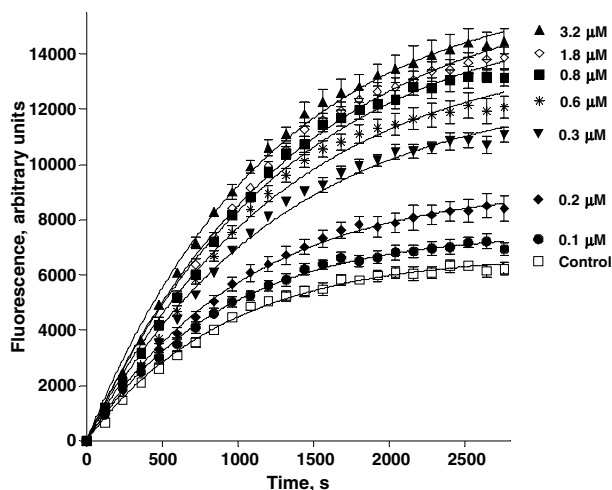
$6.49 \pm 0.08$  and  $n_H = 1.96 \pm 0.53$ . Thus, both assay types lead to the same result.

Figure 3 displays fluorescence time curves of Hoechst 33342 in buffer without cells (open squares) in A2780 (open circles) or A2780adr cells (closed squares) preincubated with 5  $\mu$ M of the compound WK-X-34. This modulator concentration fully inhibits P-gp function.<sup>16</sup> Referring to the fluorescence–time curve of A2780adr cells (closed squares) a concomitant increase in fluorescence was observed that approached the level of the wild type cell line A2780. In contrast to the fluorescence–time curve of the buffer (open squares), the fluorescence of A2780 and A2780adr cells (preincubated with WK-X-34) was comparable.



**Figure 3.** Comparison of different fluorescence–time curves of Hoechst 33342 (final concentration 5  $\mu$ M): Krebs–Hepes buffer without cells and without modulator (open squares), A2780adr cells, preincubated with 5  $\mu$ M WK-X-34 (closed squares), and A2780 cells without modulator (open circles).

Figure 4 illustrates typical fluorescence–time curves for different concentrations of the modulator WK-X-34. The kinetics of the increase in fluorescence follows an exponential profile. Figure 5 depicts the quasi-linear part of the different fluorescence–time curves from Figure 4. Figure 6 shows the comparison of concentration–response curves obtained with the plateau-values ( $Y_{\text{max}}$ ) or velocity constants calculated from the one-phase exponential association curves (Fig. 4) or the slopes of fluorescence increase (Fig. 5). The Hill-coefficients and  $\text{pIC}_{50}$ -values were statistically identical:  $\text{pIC}_{50}$  (linear) =  $6.53 \pm 0.04$ ,  $n_H = 1.63 \pm 0.24$ ;  $\text{pIC}_{50}$  ( $Y_{\text{max}}$ ) =  $6.58 \pm 0.04$ ,  $n_H = 2.08 \pm 0.30$ ;  $\text{pIC}_{50}$  (reciprocal velocities) =  $6.47 \pm 0.12$ ,  $n_H = 1.57 \pm 0.47$ . Thus, all three methods of data analysis are applicable. Using the initial quasi-linear part of the curve with linear



**Figure 4.** Fluorescence–time curves for different concentrations of WK-X-34 determined with the new Hoechst 33342 assay in A2780adr cells. Fluorescence–time curves were analyzed based on one-phase exponential association analysis. Data shown are averages  $\pm$  SE of a typical experiment with six replicates taken out from a series of four independent experiments.

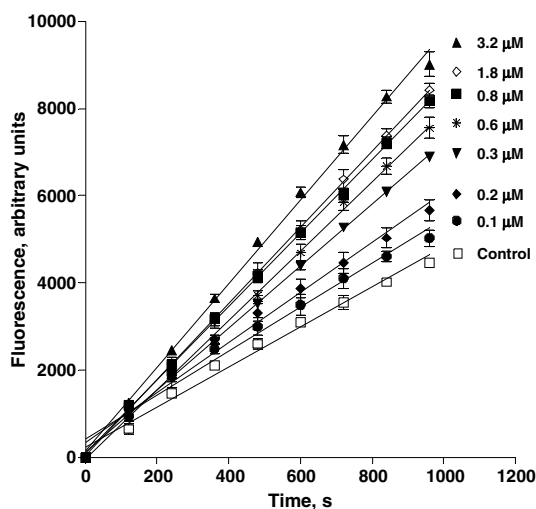


**Figure 5.** Initial part of the fluorescence–time curves for different concentrations of WK-X-34 determined with the new Hoechst 33342 assay in A2780adr cells. Slopes were determined with linear regression. Presented data are average  $\pm$  SE from one typical experiment with six replicates belonging to a series of four independent experiments.

regression saves time as it is not necessary to follow the reaction until equilibrium has been reached (Fig. 5)

Using the new assay we investigated the inhibition of the Hoechst 33342 transport by different substrates and modulators of P-gp. Table 3 summarizes the inhibitory effect of these drugs and, additionally, of three MDR modulators of the XR-type (Table 2). These compounds were selected as to represent a large variety of substances that possibly interact with different binding sites of the protein. Cyclosporine A and vinblastine have been reported to interact with P-gp in a non-competitive manner.<sup>25,26</sup> The XR-modulators and their analogue

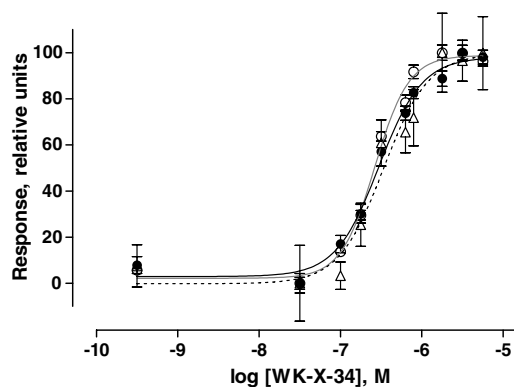


**Figure 6.** Comparison of the concentration–response curves generated for WK-X-34 in A2780adr cells with the new Hoechst 33342 assay by using: (i) linear regression analysis of the initial quasi-linear part (closed circles), (ii) the  $Y_{\max}$ -values derived from the one-phase exponential association analysis (open circles), (iii) the reciprocal velocity-values determined from one-phase exponential association fit (open triangles):  $pIC_{50}$  (linear) =  $6.53 \pm 0.04$ ,  $n_H = 1.63 \pm 0.24$ ;  $pIC_{50}$  ( $Y_{\max}$ ) =  $6.58 \pm 0.04$ ,  $n_H = 2.08 \pm 0.30$ ;  $pIC_{50}$  (reciprocal velocities) =  $6.47 \pm 0.12$ ,  $n_H = 1.57 \pm 0.47$ . Data shown are average  $\pm$  SE from one typical experiment with six replicates out of a series of four independent experiments.

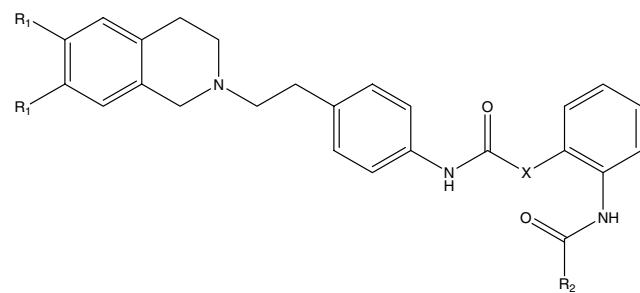
WK-X-34 are possibly interacting with the Hoechst 33342 binding site.<sup>6</sup> For nicardipine and progesterone distinct binding sites are proposed.<sup>6,27,28</sup> Verapamil, diltiazem and reserpine are well known modulators while imatinib represents a new tyrosine kinase inhibitor.<sup>29</sup> Rhodamine 123 could not be examined as it was simultaneously excited and quenched the fluorescence of Hoechst 33342 (data not shown). As seen from Table 3 the rank order of the inhibitory effects of the compounds is: progesterone < diltiazem < imatinib  $\leq$  vinblastine < verapamil  $\leq$  nicardipine < reserpine < cyclosporine A.

The above compounds together with the three 3rd generation modulators XR9456, XR9577, and WK-X-34 were also investigated in the calcein AM assay (this assay has recently been established in our laboratory<sup>30</sup>). The results are presented in Table 4. Figure 7 shows the scatterplot of the  $pIC_{50}$ -values obtained in the Hoechst 33342 and calcein AM assay. The correlation coefficient is 0.98 indicating that both assays yield significantly comparable results. The inhibitory activities of several compounds were measured by the calcein AM assay also in MDCK cells transfected with the ABCB1 gene (MDCK-MDR1).<sup>31</sup> The  $pIC_{50}$ -values are summarized in Table 4 and Figure 8 shows the scatterplot of the  $pIC_{50}$ -values determined in both cell lines. The correlation coefficient of the inhibitory potencies in the two cell lines is calculated as 0.98, clearly emphasizing that P-glycoprotein is the main mechanism which decreases the intracellular calcein AM concentration.

### 3. Discussion

The purpose of this study was to develop a functional, HTS-capable assay for P-gp activity using the substrate Hoechst 33342 and to measure in this way the P-gp



**Table 2.** Structures of the 3rd generation P-gp modulators


Compound	R <sub>1</sub>	R <sub>2</sub>	X
XR9456	OCH <sub>3</sub>	Phenyl	—
XR9577	H	3-Quinoliny	—
WK-X-34	OCH <sub>3</sub>	3,4-Dimethoxyphenyl	—
WK-X-50	H	3-Quinoliny	NH

**Table 3.** pIC<sub>50</sub>-values and Hill-coefficients of different modulators and substrates in the Hoechst assay

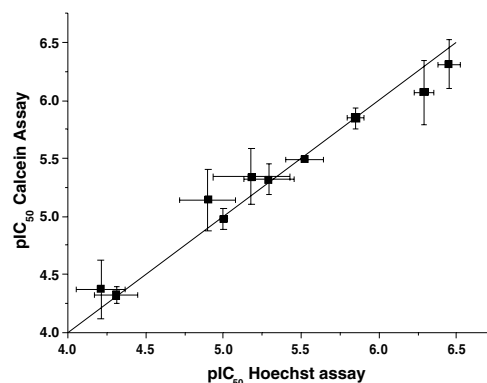
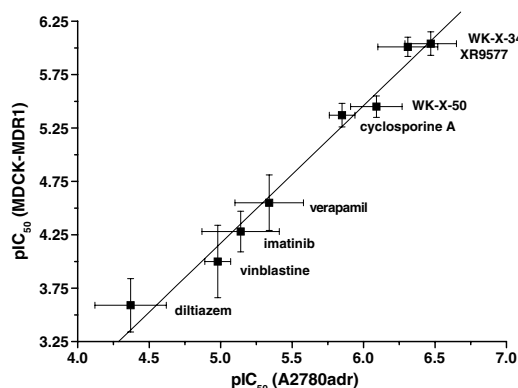
Substance	pIC <sub>50</sub> ± SD	n <sub>H</sub> ± SD
Cyclosporine A	5.85 ± 0.05	3.11 ± 0.23
Diltiazem	4.21 ± 0.16	0.89 ± 0.24
Imatinib	4.90 ± 0.18	1.38 ± 0.38
Nicardipine	5.29 ± 0.16	1.19 ± 0.43
Progesterone	4.31 ± 0.14	1.16 ± 0.15
Reserpine	5.52 ± 0.12	1.34 ± 0.28
Verapamil	5.18 ± 0.25	0.78 ± 0.08
Vinblastine	5.00 ± 0.02	2.61 ± 0.62
XR9456	6.29 ± 0.06	1.89 ± 0.35
XR9577	6.45 ± 0.07	1.89 ± 0.33
WK-X-34	6.48 ± 0.15	2.53 ± 0.47

Data shown are means ± SD.

**Table 4.** pIC<sub>50</sub>-values and Hill-coefficients of different modulators and substrates in the calcein AM assay

Substance	A2780adr		MDCK-MDR1	
	pIC <sub>50</sub> ± SD	n <sub>H</sub> ± SD	pIC <sub>50</sub> ± SD	n <sub>H</sub> ± SD
Cyclosporine A	5.85 ± 0.09	3.63 ± 1.08	5.37 ± 0.11	2.71 ± 0.36
Diltiazem	4.37 ± 0.25	1.15 ± 0.38	3.59 ± 0.25	0.77 ± 0.18
Imatinib	5.14 ± 0.27	1.18 ± 0.22	4.28 ± 0.19	1.31 ± 0.44
Nicardipine	5.32 ± 0.13	2.44 ± 0.25	—	—
Progesterone	4.32 ± 0.07	1.31 ± 0.15	—	—
Reserpine	5.49 ± 0.09	1.88 ± 0.32	—	—
Verapamil	5.34 ± 0.24	0.87 ± 0.21	4.55 ± 0.26	0.88 ± 0.22
Vinblastine	4.98 ± 0.09	2.06 ± 0.20	4.00 ± 0.34	1.50 ± 0.19
XR9456	6.07 ± 0.28	2.01 ± 0.57	—	—
XR9577	6.31 ± 0.21	2.42 ± 0.87	6.01 ± 0.09	1.66 ± 0.39
WK-X-34	6.47 ± 0.18	2.89 ± 0.55	6.04 ± 0.11	2.24 ± 0.51
WK-X-50	6.09 ± 0.18	2.60 ± 0.71	5.45 ± 0.10	2.04 ± 0.39

activity in relation to the H-site. The physicochemical properties of Hoechst 33342 and its enormous milieu dependency of fluorescence intensity allowed exclusion of time-consuming washing steps. The use of the quasi-linear part of the concentration–response curves for IC<sub>50</sub> and n<sub>H</sub> determination shortened the procedure additionally. In this way the assay has been significantly simplified.

**Figure 7.** Scatterplot of the pIC<sub>50</sub>-values of the Hoechst 33342 assay and the calcein AM assay. Data shown are average ± SD of at least three independent experiments. The correlation coefficient was 0.98.**Figure 8.** Scatterplot of the pIC<sub>50</sub>-values of eight different substances obtained in the calcein AM assay. Data shown are average ± SD of at least three independent experiments. The correlation coefficient was 0.98.

The potency of eight different standard modulators and substrates and three 3rd generation MDR modulators were investigated with the new Hoechst 33342 assay and the well-known calcein AM assay (Tables 3 and 4). The correlation coefficient was 0.98 indicating a nearly perfect correlation between the two assays (Fig. 7). At a first glance this result was surprising and prompted us to search for functional assay studies involving more than one P-gp substrate.

Wang et al. analyzed the potency of a larger number of inhibitors to decrease the P-gp mediated efflux of three different fluorescent substrates (daunorubicin, LDS-751, and rhodamine 123) from MDR1 overexpressing cells (Table 5).<sup>32</sup> Six of these compounds (vinblastine, verapamil, nicardipine, cyclosporine A, reserpine, and progesterone) were identical to those tested by us. For these compounds, a PCA was performed to estimate the multiple intercorrelation between the five assays and to possibly reveal the internal structuring of the data.<sup>33,34</sup> The PCA results are given in Table 6. The first PCA is based only on the activity data of Wang et al. From our data it is not apparent that the interaction between the inhibitors and the substrates doxorubicin (D), LDS-751 (L), and rhodamine 123 (R) is unique as

**Table 5.** P-gp inhibition data taken from Wang et al.<sup>32</sup> using the following P-gp substrates: daunorubicin (*D*), LDS-751 (*L*), and rhodamine 123 (*R*)

Substance	<i>D</i>	<i>L</i>	<i>R</i>	p <i>K</i> <sub>m</sub> ATPase <sup>47</sup>	p <i>K</i> <sub>m</sub> ATPase <sup>49</sup>
Reserpine	6.30	5.68	5.41	7.00	6.52
Dipyridamol	4.64	4.63	4.46	6.40	—
Terfenadine	5.74	5.60	5.57	5.66	—
Verapamil	5.38	5.33	5.19	5.60	6.30
Quinidine	4.73	6.00	4.47	5.30	—
Progesterone	4.02	4.06	3.72	4.76	5.30
Trifluoperazine	5.14	5.20	4.96	5.19	5.44
Tamoxifen	5.19	4.92	4.50	7.00	—
Fluphenazine	5.19	5.24	4.98	4.95	—
Cyclosporine A	5.85	5.74	5.77	7.22	7.70
Vinblastine	4.75	4.70	4.53	5.89	—
Nicardipine	5.49	5.25	4.59	—	—
Diltiazem	—	—	—	—	5.46
Chlorpromazine	—	—	—	—	5.24
<i>cis</i> -Flupentixol	—	—	—	—	5.52
Glivec	—	—	—	—	5.54

p*K*<sub>m</sub> values (ATPase assay) are taken from Litman et al.<sup>47</sup> and Gatlik-Landwojtowicz et al.<sup>49</sup>

**Table 6.** Results for different principal component analysis (PCA) using pIC<sub>50</sub>-values of six compounds determined in the five different assays: daunorubicin (*D*), LDS-751 (*L*), rhodamine 123 (*R*), Hoechst 33342 (*H*), calcein AM (*C*)

Assays	Total variance (1st PC) (%)	Eigenvalue (1st PC)	Factor loadings
<i>D</i> + <i>L</i> + <i>R</i>	95.93	2.88	<i>D</i> = 0.975, <i>L</i> = 0.995, <i>R</i> = 0.968
<i>D</i> + <i>L</i> + <i>R</i> + <i>H</i>	95.53	3.82	<i>D</i> = 0.967, <i>L</i> = 0.995, <i>R</i> = 0.969, <i>H</i> = 0.979
<i>D</i> + <i>L</i> + <i>R</i> + <i>C</i>	95.79	3.83	<i>D</i> = 0.965, <i>L</i> = 0.997, <i>R</i> = 0.971, <i>C</i> = 0.983
<i>D</i> + <i>L</i> + <i>R</i> + <i>H</i> + <i>C</i>	95.85	4.79	<i>D</i> = 0.959, <i>L</i> = 0.994, <i>R</i> = 0.969, <i>H</i> = 0.984, <i>C</i> = 0.988

proposed by Wang et al. The first principal component (PC1) explains more than 95% of the variance in activity (Table 6). Separate PCAs using pIC<sub>50</sub>-values obtained by Wang et al. and our pIC<sub>50</sub>-values determined in the Hoechst 33342 (*H*) and the calcein AM (*C*) assay lead to the same result: PC1 describes more than 95% of the total variance. The same holds true if both assays are taken into account (Table 6). This is to be expected considering as *H* and *C* assays are highly intercorrelated (Fig. 7). In general, the PCA results indicate a strong multiple intercorrelation among the biological data obtained with the different functional assays.

These results raise the question if the biological activity data measured in different functional assays possibly correlate ‘always’? To further address this question we analyzed by PCA the available biological data of substrates and inhibitors of P-gp examined in different functional assays.<sup>35–41</sup> Table 7 contains the results of pair wise and multiple correlations for different data sets taken from the literature. Most of these functional assays, using different substrates, show a good to excellent correlation. This observation seems to be surprising as the different substrates vary in their structural properties and may presumably interact with different binding sites of P-gp.

Using the simplest models for competitive, non-competitive, and un-competitive inhibition from enzyme kinetics, the dependence of the expected IC<sub>50</sub>-value on the type of inhibition was analyzed. For a non-competitive inhibitor, the ratio of IC<sub>50</sub> to the inhibition constant *K*<sub>i</sub> should be constant and independent of the reduced

substrate concentration *S*' as defined by the relationship  $S' = S/K_m$ . In this equation, *S* is the substrate concentration and *K*<sub>m</sub> is the Michaelis–Menten constant. For a competitive inhibitor the ratio should increase as:  $IC_{50}/K_i = 1 + S'$ . The un-competitive inhibition type is characterized by the relationship of  $IC_{50}/K_i = 1/S'$ .<sup>42</sup> Considering the assay conditions the substrate concentrations are most probably below *K*<sub>m</sub>. In the calcein AM assay a substrate concentration of 0.25 μM is applied and measurements up to a fivefold higher concentration led to a linear increase in fluorescence intensity, indicating that the used concentration is well below the *K*<sub>m</sub> of calcein AM. In the Hoechst 33342 assay no saturation was observed at concentrations of Hoechst 33342 up to 30 μM (data not shown). Obviously, if the substrate concentration is below its *K*<sub>m</sub>, competitive and non-competitive inhibitors will behave very similar. Even when the substrate concentration approaches *K*<sub>m</sub> of the compound the calculated difference of IC<sub>50</sub>-values becomes only two, or 0.3 log units, for a competitive versus a non-competitive inhibitor. Therefore, a similar potency (IC<sub>50</sub>) can be expected regardless of whether an inhibitor interacts with a P-gp substrate in a competitive or in a non-competitive way. Only un-competitive inhibitors are expected to differ, as long as the substrate concentration is low compared to their *K*<sub>m</sub>. The correct model is certainly more complex, because allosteric interactions have been reported in the literature. However, their influence on the IC<sub>50</sub>-values is estimated to be small in most cases as illustrated by the following examples. The mutual stimulation of Hoechst 33342 and rhodamine 123 transports was reported to be only in the range of two to three.<sup>4</sup> For the interaction of Hoe-

**Table 7.** Comparison of different assays by principal component analysis

Reference	No. of compounds	Correlation
Leonessa et al. <sup>35</sup> Four analogues of progesterone, progesterone, verapamil, and cyclosporine A were investigated with [ <sup>3</sup> H]vinblastine and doxorubicin accumulation assays in P-gp overexpressing cells	7	Explained variance: 99.2% Factor loadings > 0.99
Lee et al. <sup>38</sup> The anti-MDR1 activity data of HIV-1 protease inhibitors and cyclosporine A were obtained in five different assays: daunorubicin, rhodamine 123, bodipy-FL-verapamil, bodipy-FL-vinblastine, bodipy-FL-prazosine	4	Explained variance: 82.4% Factor loadings > 0.85
Ecker et al. <sup>40</sup> and Chiba et al. <sup>41</sup> The pIC <sub>50</sub> -values of 28 propafenone-analogues were determined with the MTT and rhodamine 123 assay using P-gp overexpressing cells	28	Explained variance: 92.8% Factor loadings > 0.96
Wang et al. <sup>32</sup> A set of 24 different substances were investigated in a daunorubicin, LDS-751, and rhodamine 123 assay using P-gp overexpressing cells	24	Explained variance: 89.5% Factor loadings > 0.93
Ekens et al. <sup>36</sup> Seventeen structurally diverse compounds were investigated in a [ <sup>3</sup> H]vinblastine accumulation and calcein AM assay	17	Explained variance: 90.8% Factor loadings > 0.95
Ecker et al. <sup>37</sup> Using a daunorubicin and rhodamine 123 efflux assay to detect the potency of 12 propafenone-analogues in a MDR1 overexpressing cell line	12	Explained variance: 99.5% Factor loadings > 0.99
Boer et al. <sup>39</sup> Dexniguldipine, B9203-016, PSC833 and GF120918 were investigated using the following three substrates: rhodamine 123, [ <sup>3</sup> H]daunorubicin, [ <sup>3</sup> H]vincristine	4	Explained variance: 94.1% Factor loadings > 0.94

For the PCA, the following parameters are given: (i) total variance explained by the 1st principal component and (ii) the factor loadings of the 1st PC.

chst 33342 and LDS-751, an even smaller stimulation by a factor of 1.6 was observed.<sup>43</sup> Lugo and Sharom described negative cooperativity between rhodamine 123 and LDS-751.<sup>44</sup> The cooperativity factor was calculated as about 5, but the maximum interaction was achieved only at high drug concentrations. In all cases, the allosteric interaction was so weak, that the pIC<sub>50</sub>-values were not influenced significantly. In summary, the measurement of IC<sub>50</sub> at a fixed substrate concentration well below its *K<sub>m</sub>* is unsuitable to distinguish between the types of interaction. This can possibly explain the similar behavior of the same substrates and modulators in the different functional assays.

If a modulator inhibits the P-gp function, the efflux of substrates will decrease independently of the site specificity. The controversial results reported in the literature for the XR-analogues can be interpreted in this context. According to Martin et al.<sup>6</sup> they bind to the H-site and if they block the P-gp transport, this will increase the daunorubicin accumulation no matter what site daunorubicin may interact with, presumably the R-site.<sup>4</sup> Our recent studies on structure–activity relationships of XR-compounds showed that parts of their structures that overlap with the Hoechst 33342 structure can be re-

lated to the ability of the compounds to bind to the same site on P-gp as the substrate does. The parts of the structures that have no correspondence to the structure of Hoechst 33342 can be involved in additional interactions and thus can presumably be attributed to their inhibitory effect on the protein function.<sup>45</sup> However, whether these interactions interfere with the R-site or other binding sites remain to be established. This is directly related to the question when these interactions take place: before the rearrangement of the transmembrane domains of P-gp from the ATP-free to the ATP-bound functional state or at some of the next steps in the transport cycle of the protein.<sup>46</sup>

But do all functional assays lead to significantly comparable results? To answer this question we compared the results obtained in the Hoechst and calcein AM assays with literature data obtained in the ATPase activity assay of P-gp. The p*K<sub>m</sub>* values for ATPase stimulation, taken from Litman et al.,<sup>47</sup> were compared by PCA with the pIC<sub>50</sub>-values of Wang et al. for 11 structurally unrelated substances (Table 8). While for the three functional assays of Wang et al. high factor loadings in PC1 are obtained, the factor loading of the ATPase activity assay is far lower, showing its deviating behav-

**Table 8.** Results for different principal component analysis

Assays ( <i>n</i> = 11)	Total variance (1st PC) (%)	Eigenvalue (1st PC)	Factor loadings
<i>D</i> + <i>L</i> + <i>R</i>	86.41	2.59	<i>D</i> = 0.950, <i>L</i> = 0.877, <i>R</i> = 0.960
<i>D</i> + <i>L</i> + <i>R</i> + ATPase	72.32	2.89	<i>D</i> = 0.966, <i>L</i> = 0.823, <i>R</i> = 0.940, ATPase = 0.590

The PCA are based on the pIC<sub>50</sub>-values obtained in different assays: daunorubicin (*D*), LDS-751 (*L*), rhodamine 123 (*R*) data are taken from Wang et al.<sup>32</sup> and the p*K<sub>m</sub>* values of 11 different compounds are taken from Litman et al.<sup>47</sup> (ATPase).

ior. The extraction of PC2 followed by Varimax rotation clearly shows the difference between the functional assays and the ATPase test system. The first eigenvalue drops from 2.89 (Table 8) to 2.39 and the second one increases to 1.28. Also the factor loadings support this observation, as PC2 is exclusively loaded by the ATPase data (factor loading = 0.97). Although with a smaller number of compounds in common, two other data sets with ATPase activity were also compared. ATPase activity data of four compounds were taken from Xia et al.<sup>48</sup> A pair wise correlation consisting of the  $pK_m$  values for progesterone (4.31), vinblastine (5.80), verapamil (4.76), and cyclosporine A (8.00) and the  $pIC_{50}$ -values of the Hoechst 33342, and the calcein AM assay, respectively, revealed moderate correlations of  $R^2 = 0.76$  for Hoechst 33342 and ATPase and  $R^2 = 0.66$  for the calcein AM and ATPase data. Of course, the analysis included only four substances. Another comparison involving six and nine compounds was performed with the ATPase activities determined by Gatlik-Landwojtowicz et al.<sup>49</sup> Again moderate intercorrelations were found with the ATPase data:  $R^2 = 0.85$  for Hoechst 33342 ( $n = 6$ ) and  $R^2 = 0.56$  for calcein AM ( $n = 9$ ).

These results may indicate that ATPase activity data expressed as  $pK_m$  values show a different structural dependency compared to  $pIC_{50}$ -values obtained in the functional efflux or influx assays. The Hoechst 33342 and calcein AM assay or other P-gp substrate-based efflux or influx test systems could generally be characterized as competition assays between the transported substrate and the investigated drug. In contrast the  $pK_m$  value determined in the ATPase activity assay describes the affinity of the analyzed compound to P-gp, thus presenting another type of the P-gp assay.

In conclusion, a new Hoechst assay to assess the potency of modulators and substrates interacting with the H-site of P-gp was developed. The analysis of the  $pIC_{50}$ -values obtained by this and other functional transport assays shows only weak comparability with ATPase activity data and underlines the importance of both assay types for the characterization of different ABC-transporters.

## 4. Experimental

### 4.1. Chemicals

Docetaxel, oxaliplatin, and vinblastine were kindly provided by Merlin-Apotheke (Bonn, Germany). Doxorubicin was a gift from Medac (Hamburg, Germany). Cisplatin and MTT were purchased from Acros (Fairlawn, NJ, USA). All other chemicals were purchased from Sigma Chemicals (Taufkirchen, Germany) unless otherwise stated.

### 4.2. Cell culture

Human ovarian carcinoma cell lines A2780 and the corresponding adriamycin-resistant A2780adr cell line were purchased from ECACC (European collection of animal cell cultures, No. 93112520 [A2780adr] and No.

93112519 [A2780], United Kingdom). Cells were cultivated in RPMI-1640 medium supplemented with 10% fetal bovine serum, 50  $\mu$ g/ml streptomycin, 50 U/ml penicillin G, and 365  $\mu$ g/ml L-glutamine (Sigma Chemicals). Cells were grown at 37 °C in a humidified atmosphere containing 5% CO<sub>2</sub>. Cells were grown to 80–90% confluence and treated with trypsin–EDTA before subculturing. Every 5th passage doxorubicin (0.1  $\mu$ M final concentration) was added to the cell culture medium of A2780adr cells to maintain a selection/resistance pressure and to conserve P-gp overexpression.

### 4.3. Cytotoxicity assay

The cytotoxicity assays were carried out in A2780 and A2780adr cells. Cells were harvested by brief trypsinization, and seeded into 96-well plates at a density of 10,000 cells. The cytotoxic compounds were added in various concentrations and incubated for 72 h at 37 °C and 5% CO<sub>2</sub>. After 72 h, cytotoxicity was assessed using the MTT assay as follows: cells were incubated with 20  $\mu$ l of a 5 mg/ml MTT solution for 70 min, and then solubilized with a 2-propanol/HCl-mixture (1:300). The absorption of the solubilized formazan was measured at 595 nm (test wavelength) and 690 nm (reference wavelength) applying a POLARstar microplate reader (BMG Labtechnologies, Offenburg, Germany). Absorption at the reference wavelength was subtracted from the absorption of the test wavelength.<sup>50</sup>

### 4.4. P-Glycoprotein surface expression

To analyze the P-gp surface expression level, cells were trypsinized as described above and counted.  $1 \times 10^6$  cells were prepared for antibody staining by washing. After three washing steps with KHP, cells were first rinsed with ice-cold washing-buffer (PBS, 0.5% BSA) and then dissolved in ice-cold staining buffer (PBS, 0.5% BSA, 0.1% NaN<sub>3</sub>). To the staining buffer, 20  $\mu$ l of the FITC-labeled monoclonal anti-human P-gp antibody (BD Biosciences, USA) was added. Cells were protected from light and incubated for 40 min on ice. After the incubation period, cells were washed again with staining buffer and then resuspended into the washing-buffer. The binding of the FITC-labeled P-gp antibody was analyzed with a flow cytometer (FACS Calibur, Becton Dickinson, and Heidelberg, Germany). Fluorescence was measured by counting 10,000 events with an excitation wavelength of 488 nm and an emission wavelength of 530/15 nm—the band pass filter for FITC (FL1). Gates were set to forward and sideward scatter to exclude damaged cells and cell debris. Autofluorescence of A2780adr and A2780 cells were tested and found to be comparable. Data were quantified using the Cell Quest Pro software. At least five independent experiments were performed. The geometric means of the fluorescence were applied to determine the *MDR1* expression status of the different cell lines.

### 4.5. Standard Hoechst 33342 assay

Cells were grown in T75- or T175-flasks. At a confluence of approximately 80% cells were harvested by trypsin-



tion (0.05% trypsin/0.02% EDTA). Pelleted cells were resuspended in fresh culture medium and counted with a Casy I Modell TT cell counter (Schaefer System GmbH, Reutlingen, Germany). After three washing steps with Krebs–Hepes buffer, cells were seeded into black 96-well plates (Greiner, Frickenhausen, Germany) at a density of approximately 30,000 cells in a volume of 90  $\mu$ l per well. Then, 10  $\mu$ l of various test compounds in different concentrations were added, resulting in a final volume of 100  $\mu$ l per well. The prepared 96-well plates were kept under 5% CO<sub>2</sub> at 37 °C for 30 min. After this preincubation period, 20  $\mu$ l of a 30- $\mu$ M Hoechst 33342 solution which was protected from light were added to each well.

Subsequently, fluorescence was measured immediately at constant time intervals (120 s) up to 46 min at an excitation wavelength of 365 nm and an emission wavelength of 450 nm using a 37 °C tempered BMG POLARstar microplate reader.

#### 4.6. Fluorescence microscopy

Cells were grown as described above, harvested, and washed three times with KHP. Three million cells were stained with Hoechst 33342 (final concentration: 5  $\mu$ M) for 20 min. After loading the cells with Hoechst 33342, the cells were not washed again. Cells were viewed under microscope (Microscope Axiovert 25, Zeiss, Jena, Germany). Images were captured using 360/40 and 460/20 filters for excitation and emission, respectively.

#### 4.7. Data analysis

Statistical analyses were performed using SPSS (version 12.0 for Windows). Absorption or fluorescence data were normalized as follows: the lowest measured value was subtracted from all data points setting it to zero. The highest measured value was defined as 100%, and all other data were normalized within this range.

#### 4.8. New Hoechst assay of P-gp substrates and inhibitors

The 96-well plate was divided into two parts: the main part including 64 wells was provided with cells, the second part containing the remaining 32 wells was only filled up with Krebs–Hepes buffer. The 33 wells localized in the 1st, 4th, 7nd, and 10th column of the 12 columns of the 96-well plate were defined as ‘background’ wells. Each modulator or substrate concentration was added to three wells containing one ‘background’ well and two wells including cells. The fluorescence measured in the ‘background’ wells was subtracted from the fluorescence measured in the corresponding wells which were supplemented with cells. These data were used for the following analyses.

Three different ways to analyze the fluorescence data obtained with the Hoechst assay were applied: (i) The upper plateau-value,  $Y_{\max}$ -value, of each fluorescence–time curve was determined based on one-phase exponential curve fitting. The obtained  $Y_{\max}$ -values were used as a relative measure of P-gp activity. (ii) The reciprocal velocity-values derived from one-phase exponential

curve fitting. (iii) The slope of each fluorescence–time curve consisting of fluorescence-data points measured up to 16 min was calculated by linear regression and used as dependent parameter. From either of these values, concentration–response curves were generated by non-linear regression using the 4-parameter logistic equation with variable Hill slope (GraphPad Prism 3.0 software, San Diego, CA). IC<sub>50</sub> is the concentration of the modulator or substrate yielding an increase of 50% of the fluorescence–time curve slope or an increase of 50% of the  $Y_{\max}$ -value, respectively.

Under the assay conditions with sub-saturating substrate concentrations, the ratio of intracellular ( $c_{\text{in}}$ ) to extracellular ( $c_{\text{out}}$ ) substrate concentration depends on the ratio of pumping speed to the rate of passive diffusion ( $k^*$ ) as follows:

$$\frac{c_{\text{in}}}{c_{\text{out}}} = \frac{1}{1 + k^*} = \frac{\text{Bottom}}{\text{Top}}$$

For the development of this relationship, see for example, Ref.51 Bottom corresponds to the minimal fluorescence with no inhibition of P-gp and Top denotes the maximal fluorescence obtained with full inhibition of P-gp. Thus, the determined IC<sub>50</sub>-values agree with 50% inhibition of P-gp only at very high pump rates compared to the speed of passive diffusion and therefore have to be considered as apparent inhibition constants.

As long as the expression and resistance levels remain constant, the apparent IC<sub>50</sub>-values can be used for comparative purposes.

#### Acknowledgment

I.K. Pajeva thanks the NSF-Bulgaria for financial support (Grant L-1416).

#### References and notes

- Schinkel, A. H.; Jonker, J. W. *Adv. Drug Deliv. Rev.* **2003**, 55, 3–29.
- Hoffmann, U.; Kroemer, H. K. *Drug Metab. Rev.* **2004**, 36, 669–701.
- Lee, C. H. *Curr. Med. Chem. Anticancer Agents* **2004**, 4, 53–62.
- Shapiro, A. B.; Ling, V. *Eur. J. Biochem.* **1997**, 250, 130–137.
- Kondratov, R. V.; Komarov, P. G.; Becker, Y.; Ewenson, A.; Gudkov, A. V. *Proc. Natl. Acad. Sci. U.S.A.* **2001**, 98, 14078–14083.
- Martin, C.; Berridge, G.; Higgins, C. F.; Mistry, P.; Charlton, P.; Callaghan, R. *Mol. Pharmacol.* **2000**, 58, 624–632.
- Roe, M.; Folkes, A.; Ashworth, P.; Brumwell, J.; Chima, L.; Hunjan, S.; Pretswell, I.; Dangerfield, W.; Ryder, H.; Charlton, P. *Bioorg. Med. Chem. Lett.* **1999**, 9, 595–600.
- Loo, T. W.; Clarke, D. M. *J. Membr. Biol.* **2005**, 206, 173–185.
- Pleban, K.; Kopp, S.; Csaszar, E.; Peer, M.; Hrebicek, T.; Rizzi, A.; Ecker, G. F.; Chiba, P. *Mol. Pharmacol.* **2005**, 67, 365–374.

10. Pajeva, I.; Wiese, M. *J. Med. Chem.* **2002**, *45*, 5671–5686.
11. Spoelstra, E. C.; Dekker, H.; Schuurhuis, G. J.; Broxterman, H. J.; Lankelma, J. *Biochem. Pharmacol.* **1991**, *41*, 349–359.
12. Bakker, M.; Renes, J.; Groenhuijzen, A.; Visser, P.; TimmerBosscha, H.; Muller, M.; Groen, H. J. M.; Smit, E. F.; deVries, E. G. E. *Int. J. Cancer* **1997**, *73*, 362–366.
13. Sasaki, H.; Takada, K.; Terashima, Y.; Ekimoto, H.; Takahashi, K.; Tsuruo, T.; Fukushima, M. *Gynecol. Oncol.* **1991**, *41*, 36–40.
14. Manetta, A.; Gamboa, G.; Nasser, A.; Podnos, Y. D.; Emma, D.; Dorion, G.; Rawlings, L.; Carpenter, P. M.; Bustamante, A.; Patel, J.; Rideout, D. *Gynecol. Oncol.* **1996**, *60*, 203–212.
15. de Jong, M. C.; Slootstra, J. W.; Scheffer, G. L.; Schroeijs, A. B.; Puijk, W. C.; Dinkelberg, R.; Kool, M.; Broxterman, H. J.; Melloen, R. H.; Scheper, R. J. *Cancer Res.* **2001**, *61*, 2552–2557.
16. Jekerle, V.; Klinkhammer, W.; Scollard, D. A.; Breitbach, K.; Reilly, R. M.; Piquette-Miller, M.; Wiese, M. *Int. J. Cancer* **2006**, *119*, 414–422.
17. Aihara, M.; Aihara, Y.; Schmidwolf, G.; Schmidwolf, I.; Sikic, B. I.; Blume, K. G.; Chao, N. J. *Blood* **1991**, *77*, 2079–2084.
18. Okochi, E.; Iwahashi, T.; Tsuruo, T. *Leukemia* **1997**, *11*, 1119–1123.
19. Minderman, H.; Suvannasankha, A.; O'Loughlin, K. L.; Scheffer, G. L.; Scheper, A. J.; Robey, R. W.; Baer, M. R. *Cytometry* **2002**, *48*, 59–65.
20. Wiese, M.; Pajeva, I. K. *Curr. Med. Chem.* **2001**, *8*, 685–713.
21. Tawar, U.; Jain, A. K.; Dwarakanath, B. S.; Chandra, R.; Singh, Y.; Chaudhury, N. K.; Khaitan, D.; Tandon, V. *J. Med. Chem.* **2003**, *46*, 3785–3792.
22. Tawar, U.; Jain, A. K.; Chandra, R.; Singh, Y.; Dwarakanath, B. S.; Chaudhury, N. K.; Good, L.; Tandon, V. *Biochemistry* **2003**, *42*, 13339–13346.
23. Shapiro, A. B.; Ling, V. *J. Biol. Chem.* **1995**, *270*, 16167–16175.
24. Shapiro, A. B.; Ling, V. *J. Bioenerg. Biomembr.* **1995**, *27*, 7–13.
25. Ayes, S.; Shao, Y. M.; Stein, W. D. *Biochim. Biophys. Acta* **1996**, *1316*, 8–18.
26. Shao, Y. M.; Ayes, S.; Stein, W. D. *Biochim. Biophys. Acta* **1997**, *1360*, 30–38.
27. Safa, A. R. *Curr. Med. Chem. Anticancer Agents* **2004**, *4*, 1–17.
28. Shapiro, A. B.; Fox, K.; Lam, P.; Ling, V. *Eur. J. Biochem.* **1999**, *259*, 841–850.
29. Druker, B. J. *Drugs* **2001**, *61*, 1775–1776.
30. Muller, H.; Klinkhammer, W.; Kassack, M. U.; Eckstein, N.; Wiese, M. *Int. J. Clin. Pharmacol. Ther.* **2004**, *42*, 644–645.
31. The MDCK-MDR1 cell line was kindly provided by Dr. P. Borst, Netherlands Cancer Institute, Amsterdam, The Netherlands.
32. Wang, E. J.; Casciano, C. N.; Clement, R. P.; Johnson, W. W. *Biochem. Biophys. Res. Commun.* **2001**, *289*, 580–585.
33. Lykouras, L.; Oulis, P.; Psarros, K.; Daskalopoulou, E.; Botsis, A.; Christodoulou, G. N.; Stefanis, C. *Eur. Arch. Psychiatry Clin. Neurosci.* **2000**, *250*, 93–100.
34. Okin, P. M.; Devereux, R. B.; Fabsitz, R. R.; Lee, E. T.; Galloway, J. M.; Howard, B. V. *Circulation* **2002**, *105*, 714–719.
35. Leonessa, F.; Kim, J. H.; Ghiorghis, A.; Kulawiec, R. J.; Hammer, C.; Talebian, A.; Clarke, R. *J. Med. Chem.* **2002**, *45*, 390–398.
36. Ekins, S.; Kim, R. B.; Leake, B. F.; Dantzig, A. H.; Schuetz, E. G.; Lan, L. B.; Yasuda, K.; Shepard, R. L.; Winter, M. A.; Schuetz, J. D.; Wikel, J. H.; Wrighton, S. A. *Mol. Pharmacol.* **2002**, *61*, 964–973.
37. Ecker, G.; Huber, M.; Schmid, D.; Chiba, P. *Mol. Pharmacol.* **1999**, *56*, 791–796.
38. Lee, C. G. L.; Gottesman, M. M.; Cardarelli, C. O.; Ramachandra, M.; Jeang, K. T.; Ambudkar, S. V.; Pastan, I.; Dey, S. *Biochemistry* **1998**, *37*, 3594–3601.
39. Boer, R.; Gekeler, V.; Ulrich, W. R.; Zimmermann, P.; Ise, W.; Schodl, A.; Haas, S. *Eur. J. Cancer* **1996**, *32A*, 857–861.
40. Ecker, G.; Chiba, P.; Hitzler, M.; Schmid, D.; Visser, K.; Cordes, H. P.; Csolle, J.; Seydel, J. K.; Schaper, K. J. *J. Med. Chem.* **1996**, *39*, 4767–4774.
41. Chiba, P.; Ecker, G.; Schmid, D.; Drach, J.; Tell, B.; Goldenberg, S.; Gekeler, V. *J. Mol. Pharmacol.* **1996**, *49*, 1122–1130.
42. Segel, I. H. *Enzyme Kinetics*; John Wiley and Sons: New York, 1976.
43. Shapiro, A. B.; Ling, V. *Eur. J. Biochem.* **1998**, *254*, 181–188.
44. Lugo, M. R.; Sharom, F. J. *Biochemistry* **2005**, *44*, 14020–14029.
45. Globisch, C.; Pajeva, I. K.; Wiese, M. *Bioorg. Med. Chem.* **2006**, *14*, 1588–1598.
46. Pajeva, I. K.; Globisch, C.; Wiese, M. *J. Med. Chem.* **2004**, *47*, 2523–2533.
47. Litman, T.; Zeuthen, T.; Skovsgaard, T.; Stein, W. D. *Biochim. Biophys. Acta* **1997**, *1361*, 159–168.
48. Xia, G. Q.; Xiao, G.; Liu, N.; Pimprale, S.; Fox, L.; Patten, C. J.; Crespi, C. L.; Miwa, G.; Gan, L. S. *Mol. Pharm.* **2006**, *3*, 78–86.
49. Gatlik-Landwojtowicz, E.; Äänismaa, P.; Seelig, A. *Biochemistry* **2006**, *45*, 3020–3032.
50. Mueller, H.; Kassack, M. U.; Wiese, M. *J. Biomol. Screen.* **2004**, *9*, 506–515.
51. Garnier-Suillerot, A.; Marbeuf-Gueye, C.; Salerno, N.; Loetchutin, C.; Fokt, I.; Krawczyk, M.; Kowalczyk, T.; Priebe, W. *Curr. Med. Chem.* **2001**, *8*, 51–64.